Strain-induced interface reconstruction in epitaxial heterostructures

N. Lazarides,[1,2] V. Paltoglou,[1,2] P. Maniadis,[1,2] G. P. Tsironis,[1,2] and C. Panagopoulos[1,2,3]

[1]*Department of Physics, University of Crete, P. O. Box 2208, GR-71003 Heraklion, Greece*

[2]*Institute of Electronic Structure and Laser, Foundation for Research and Technology-Hellas, P.O. Box 1527, GR-71110 Heraklion, Greece*

[3]*Division of Physics and Applied Physics, Nanyang Technological University 637371, Singapore*

(Received 24 November 2011; published 14 December 2011)

We investigate in the framework of Landau theory the distortion of the strain fields at the interface of two dissimilar ferroelastic oxides that undergo a structural cubic-to-tetragonal phase transition. Simple analytical solutions are derived for the dilatational and the deviatoric strains that are valid over the entire heterostructure. The solutions reveal that the dilatational strain exhibits compression close to the interface, which may in turn affect the electronic properties in that region.

DOI: 10.1103/PhysRevB.84.245428 PACS number(s): 73.40.−c, 73.21.Cd, 71.27.+a, 81.30.Kf

I. INTRODUCTION

Recent discoveries in material science related to several unexpected properties of epitaxial heterostructures made of different transition metal oxide (TMO) materials bring in the forefront of interest the problem of interface reconstruction through the development of spontaneous strain at the interface.[1,2] Lattice distortion close to the interface is known to result in a charge redistribution that leads to the formation of a two-dimensional electron gas (2DEG) and metallicity in that region.[3–6] Most of the TMOs of interest are ferroelastics that undergo structural transitions[7] from a cubic/pseudocubic to a lower symmetry phase with decreasing temperature. Notably, heterostructures containing strontium titanate ($SrTiO_3$), a band-insulator oxide undergoing a cubic-to-tetragonal (CTT) structural transition at $T_s \sim 105\,^{\circ}$K, exhibit extraordinary interfacial properties below T_s; metallicity,[1,3,6,8] superconductivity,[9] and the nonlinear Hall effect.[10] Moreover, in $LaTiO_3/SrTiO_3$ and $LaAlO_3/SrTiO_3$ heterostructures, the structural transition of $SrTiO_3$ causes the overlayers to stabilize in a tetragonal phase with an in-plane lattice constant almost equal to that of $SrTiO_3$ close to the interface.[11,12]

It has been discussed in the past that the electromagnetic properties of TMOs couple to the elastic degrees of freedom.[13–15] The effect of the tensile and compressive strains to the electronic conduction properties at the interface of TMO heterostructures has already been addressed experimentally.[16,17] Furthermore, strong polarization enhancement in ferroelectric TMO superlattices driven by interfacial strain has been unambiguously observed.[18] In the present work we apply continuous elasticity theory through a Ginzburg-Landau description in terms of the strain tensor components to a heterostructure. Based solely on symmetry considerations, Ginzburg-Landau theory can provide a reliable description of the equilibrium behavior of a system near a phase transition. It has been recently used to show theoretically the emergence of a multiferroic state of a $EuTiO_3$ film on $(LaAlO_3)_{0.29}(SrAl_{1/2}Ta_{1/2}O_3)_{0.71}$ (LSAT) substrate,[19] to provide a physical understanding of the strain-induced metal-insulator phase coexistence in manganites,[13] and to explain phase separation between metallic ferromagnetic and insulating charge-modulated phases.[20]

We investigate the interfacial effects on the strain state of a bilayer heterostructure, composed of dissimilar TMOs that join at a single planar interface, and propose a strain-based mechanism that may help understand the formation of a 2DEG. In particular, we obtain approximate analytical solutions for the dilatational and the deviatoric strain fields in the bilayer that exhibit spatial variation due to breaking of the uniformity. Notably, the dilatational strain field exhibits a well-defined minimum at the interface corresponding to local compression.[6] We argue that the suppression of the dilatational strain field in the interfacial region may encourage the formation of a 2DEG. The proposed strain-based mechanism does not exclude other possible mechanisms, like the orbital and/or the electronic reconstruction mechanisms.[21,22]

II. GINZBURG-LANDAU THEORY AND EQUATIONS OF MOTION

In the Lagrangian description of elasticity the symmetric strain tensor is defined as $\epsilon_{ij} = \{u_{i,j} + u_{j,i}\}/2$ $(i,j = x,y,z)$, where $u_{i,j}$ is the jth derivative of the ith component of the displacement vector $\mathbf{u}$ of a material point relative to its position in the parent phase. The six symmetry adapted strains for the CTT structural transition are defined as[23]

$$e_1 = u_{x,x} + u_{y,y} + u_{z,z}, \quad e_2 = \frac{1}{2}(u_{x,x} - u_{y,y}), \tag{1}$$

$$e_3 = \frac{1}{2\sqrt{3}}(u_{x,x} + u_{y,y} - 2u_{z,z}), \quad e_4 = \frac{1}{2}(u_{y,z} + u_{z,y}), \tag{2}$$

while e_5 and e_6 are given by e_4 with the cyclic permutation of the indices. The deviatoric strains e_2 and e_3 form the two-component order parameter (OP) of the CTT transition. Both the OP and the non-OP strains are coordinate-independent in the uniform product (tetragonal) phase in static equilibrium, with the latter customarily being set to zero. In a TMO heterostructure, where the uniformity of the product phase is broken due to the interface, all e_i's vary spatially; in that case, their second derivatives are linked through compatibility relations.[24] In a nonuniform state, the non-OP strains cannot be all set to zero. Specifically, in TMO heterostructures the dilatational strain e_1, which is concommitant to e_3 (Refs. 25 and 26), exhibits measurable compression indicating its importance in their structural properties.[6]

In ferroelasticity theory, the strain energy density $\mathcal{F}$ of a material undergoing a CTT structural transition is expanded in powers of the invariants of the strain tensor and their products

around the energy of the parent phase.[24–29] Thus, the functional $\mathcal{F}$ is expressed solely in terms of the e_i's and their spatial derivatives. Guided by previous works we adopt a functional $\mathcal{F}$ of the form

$$\begin{aligned}\mathcal{F} = &\frac{c_1}{2}e_1^2 + \frac{c_2}{2}\left(e_2^2+e_3^2\right) + \frac{c_3}{2}(e_4^2+e_5^2+e_6^2) + \frac{d_1}{2}(\nabla e_1)^2 \\ &+ \frac{d_2}{2}[(\nabla e_2)^2 + (\nabla e_3)^2] + \frac{a_1}{2}e_1^3 + \frac{a_2}{2}e_1\left(e_2^2+e_3^2\right) \\ &+ \frac{a_4}{3}e_3\left(e_3^2-3e_2^2\right) + \frac{b_1}{4}e_1^4 + \frac{b_2}{2}e_1^2\left(e_2^2+e_3^2\right) \\ &+ \frac{b_4}{4}\left(e_2^2+e_3^2\right)^2 + \frac{b_7}{2}e_1e_3\left(e_3^2-3e_2^2\right), \end{aligned} \tag{3}$$

where the Ginzburg-Landau coefficients a_1,a_2,a_4, b_1,b_2,b_4,b_7, and c_1,c_2,c_3 are related to the second-, third-, and fourth-order elastic coefficients of the parent phase, respectively, through (in Voigt notation)[30]

$$\begin{aligned} a_1 &= \frac{1}{27}\left(C_{111}+6C_{112}+2C_{123}\right), \\ a_2 &= \frac{2}{3}(C_{111}-C_{123}), \\ a_4 &= -\frac{1}{\sqrt{3}}\left(C_{111}-3C_{112}+2C_{123}\right), \\ b_1 &= \frac{1}{162}(C_{1111}+8C_{1112}+6C_{1122}+12C_{1123}), \\ b_2 &= \frac{1}{9}(C_{1111}+2C_{1112}-3C_{1123}), \\ b_4 &= \frac{1}{3}(C_{1111}-4C_{1112}+3C_{1122}), \\ b_7 &= -2\frac{\sqrt{3}}{27}(C_{1111}-C_{1112}-3C_{1122}+3C_{1123}), \\ c_1 &= \frac{1}{3}(C_{11}+2C_{12}), \\ c_2 &= 2(C_{11}-C_{12}), \end{aligned} \tag{4}$$

while d_1,d_2 are two independent strain-gradient coefficients. In accordance with the common principles of Landau theory, the critical temperature dependence of the c_2 elastic constant, $c_2 \propto (T - T_s)$, is supposed to be true close to the transition point.

In a single material at static equilibrium, the spatially homogeneous strains in the product phase are the lowest energy solutions of the conditions $\partial\mathcal{F}/\partial e_i = 0$. Neglecting the non-OP terms, the energy density landscape on the e_2-e_3 plane exhibits the familiar pattern of three degenerate minima corresponding to three different variants in the tetragonal phase (Fig. 1). Notably, a nonzero e_1 preserves the energetic degeneracy of the three variants. We are particularly interested in the variant having $e_2 = 0$; this is because TMO heterostructures are usually grown along the z direction and both materials go into a c-tetragonal phase at low temperatures.[11,12] For $e_2 = 0$, the energy landscape on the e_1-e_3 plane shown in Fig. 2 exhibits significant qualitative differences for different a_2 values. Specifically, the strain e_1 varies from positive (i.e., expansional) to negative (i.e., compressional) with decreasing the magnitude of a_2. A small a_2 absolute value is, however, expected from the principle $e_1 \ll e_2,e_3$ for all martensitic

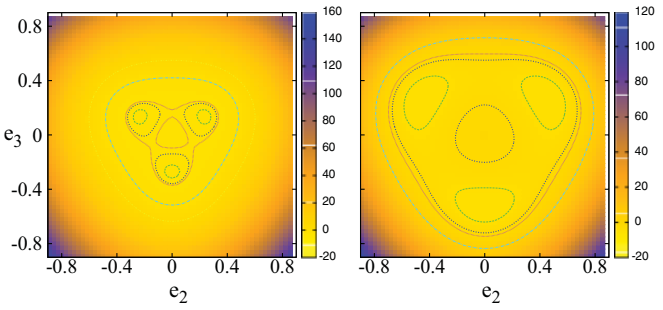

FIG. 1. (Color online) Strain energy density landscape on the e_2-e_3 plane for $a_4 = 25.4$, $b_4 = 225$, and $c_2 = -10$ (left); -50 (right), exhibiting the familiar pattern of three degenerate minima.

transformations.[28,29] Moreover, a small a_2 leads to negative e_1 and e_3, in accordance with the empirical principle for the ferroelastic transitions of close-packed solids (i.e., that the cooling of the solid is usually accompanied by a decrease of volume). The dependence of the strains on c_2 for all three variants is shown in Fig. 3 for two different values of a_2. We later refer to the two materials forming the bilayer heterostructure, which occupy the regions $z < 0$ and $z > 0$, as the left (L) and the right (R) material, respectively. The Ginzburg-Landau parameters used in Figs. 1 through 3 are those given for the left material in Table I, and they have been calculated from the corresponding elastic coefficients through Eq. (4). The second- and third-order elastic coefficients of the left material are those reported for $SrTiO_3$ (Refs. 31 and 32), while for the fourth-order ones a reasonable choice was made (Table I). Note that for the parameter a_2, which can be treated as a phenomenological one, we have also used values that are smaller than the one given in Table I for the left material (i.e., $a_2^L = -31$).

The dynamics of the displacements is governed by the Euler-Lagrange equations

$$\rho_0\ddot{u}_i = \sigma_{ik,k} + \sigma'_{ik,k}, \tag{5}$$

where

$$\sigma_{ik} \equiv \frac{\partial\mathcal{F}}{\partial u_{i,k}}, \qquad \sigma'_{ik} \equiv \frac{\partial\mathcal{R}}{\partial\dot{u}_{i,k}}, \tag{6}$$

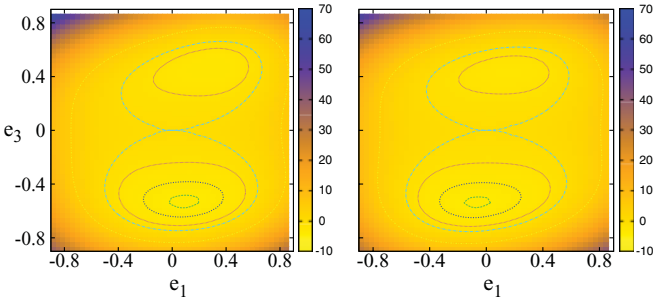

FIG. 2. (Color online) Strain energy density landscape on the e_1-e_3 plane for $c_2 = -50$, and $a_2 = -31$ (left); -10 (right). The other Ginzburg-Landau parameters are those for the left material given in Table I.

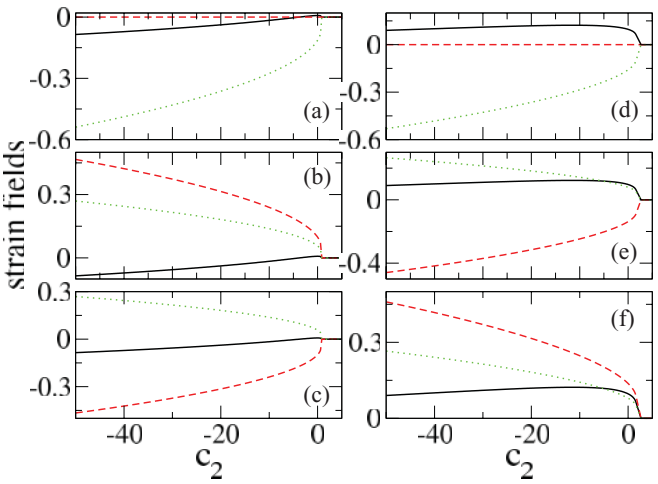

FIG. 3. (Color online) The strains e_1 (black solid line), e_2 (red-dashed line), e_3 (green-dotted line), as a function of c_2 for the three variants, for $a_2 = -7$ (left panels), -31 (right panels). The other Ginzburg-Landau parameters are those for the left material given in Table I.

are the strain tensor and the dissipative strain tensor, respectively, ρ_0 is the density in the parent phase, and $\mathcal{R}$ is the the Rayleigh dissipation function

$$\mathcal{R} = \tfrac{1}{2}c_1'\dot{e}_1^2 + \tfrac{1}{2}c_2'\left(\dot{e}_2^2 + \dot{e}_3^2\right) + \tfrac{1}{2}c_3'\left(\dot{e}_4^2 + \dot{e}_5^2 + \dot{e}_6^2\right). \quad (7)$$

Then, from Eq. (5) we get

$$\rho_0\ddot{u}_i = \partial_i\Phi_i + \tfrac{1}{2}(c_3H_i + c_3'\dot{H}_i), \quad (8)$$

where

$$H_x = e_{6,y} + e_{5,z}, \quad H_y = e_{4,z} + e_{6,x}, \quad H_z = e_{4,y} + e_{5,x}, \quad (9)$$

and

$$\Phi_i = -\nabla^2 G_i + W_i + R_i + \dot{W}_i', \quad (10)$$

$$W_i = c_1e_1 + \frac{c_2}{2}\left(qe_2 + \frac{1}{\sqrt{3}}e_3\right), \quad W_z = c_1e_1 - \frac{c_2}{\sqrt{3}}e_3, \quad (11)$$

with $q = +1(-1)$ for $i = x(y)$. The functions W_i' and G_i have the same form with that of the W_i's, with the obvious change $c_j \to c_j'$ and $c_j \to d_j$, respectively, $(j = 1,2)$, and the R_i's

TABLE I. Second-, third-, and fourth-order elastic coefficients (in units of 10^{11} N/m^2), and Ginzburg-Landau (GL) dimensionless coefficients for the left and the right material used in the calculations.

Elastic Const.	Left Mater.	Right Mater.	GL Coeff.	Left Mater.	Right Mater.
C_{11}	3.172	2.979	c_1	1.74	1.89
C_{12}	1.025	1.355	c_2	4.29	2.25
C_{111}	−50.0	−47.5	a_1	−3.00	−2.80
C_{112}	−4.0	−3.8	a_2	−31.0	−29.5
C_{123}	−3.0	−2.85	a_4	25.4	24.1
C_{1111}	777.5	760.0	b_1	48.7	42.9
C_{1112}	270.0	152.0	b_2	63.3	36.9
C_{1122}	326.0	342.0	b_4	225	393
C_{1123}	250.0	244.0	b_7	−35.4	−40.3

are lengthy nonlinear functions of e_1, e_2, and e_3, which are given in the Appendix.

III. APPROXIMATE SOLUTIONS AND INTERFACE RECONSTRUCTION

To separate the interfacial effects on the strain state of the bilayer heterostructure (from those originating from external boundaries, domain walls, dislocations, etc.), we consider two monodomain, semi-infinite TMOs joined along a chemically abrupt, planar interface at $z = 0$. Equation (8) could be simplified in a strict way since at low temperatures the strains depend on one coordinate only and $e_2 = 0$ (Refs. 33 and 34). However, for nonzero e_1 the simplification of Eq. (8) following the strict way is a nontrivial task, which makes preferable the use of a simple ansatz for the displacements. This ansatz assures that the strains depend only on the z coordinate and that e_2, as well as the small strains e_4, e_5, e_6, are identically zero. Assume that the strains exhibit a relatively strong z-coordinate dependence in the proximity of the interface, while they attain their static equilibrium values for large enough $|z|$. This approximation seems well suited for heterostuctures composed of TMOs with a small lattice mismatch (i.e., $LaTiO_3/SrTiO_3$). Indeed, both experimental observations[35] (discussed below) and first-principles calculations[4] indicate that strain inhomogeneity and lattice deformation occur within a few layers near the interface. Thus, for practical purposes, it is sufficient for the two layers of the heterostructure to be thick enough for the deformation to vanish relatively far from the interface. The choice of semi-infinite layers was made only for mathematical convenience.

We then introduce the ansatz

$$u_x = -\frac{a}{2}x, \quad u_y = -\frac{a}{2}y, \quad u_z = bz + f(z), \quad (12)$$

where $f(z)$ is an as yet unknown function, and

$$a = -\tfrac{2}{3}(e_{10} + \sqrt{3}e_{30}), \quad b = +\tfrac{1}{3}(e_{10} - 2\sqrt{3}e_{30}), \quad (13)$$

with e_{10} and e_{30} being the values of e_1 and e_3, respectively, far from the interface. The nonzero strains are then

$$e_1 = e_{10} + f'(z), \quad e_3 = e_{30} - \frac{1}{\sqrt{3}}f'(z), \quad (14)$$

where the prime denotes differentiation with respect to z. The substitution of Eq. (14) into Eq. (8) results, in the static limit, in the equation

$$\left(d_1 + \frac{d_2}{3}\right)G''' = \left(c_1 + \frac{c_2}{3}\right)G' + R_z'(G), \quad (15)$$

where $G = G(z) \equiv f'(z)$, and R_z with $e_2 = 0$ is

$$R_z = \frac{3a_1}{2}e_1^2 + b_1e_1^3 + \left(\frac{a_2}{2} - \frac{a_4}{\sqrt{3}}\right)e_3^2 + \left(\frac{b_7}{2} - \frac{b_4}{\sqrt{3}}\right)e_3^3 - \frac{1}{\sqrt{3}}e_1e_3\left[a_2 + b_2e_1 + 3\left(\frac{b_7}{2} - \frac{b_2}{\sqrt{3}}\right)e_3\right], \quad (16)$$

where e_1 and e_3 are meant to be expressed in terms of f through Eq. (14). After rearrangement, Eq. (15) becomes

$$G''' = G'(\tilde{\kappa} + 3\tilde{\lambda}G + 6\tilde{\mu}G^2), \tag{17}$$

where

$$\tilde{\kappa} = \frac{a_{1z} + \kappa}{d_{1z}}, \quad \tilde{\lambda} = \frac{\lambda}{3d_{1z}}, \quad \tilde{\mu} = \frac{\mu}{6d_{1z}}, \tag{18}$$

with

$$a_{1z} = c_1 + \tfrac{1}{3}c_2 = C_{11}, \quad d_{1z} = d_1 + \tfrac{1}{3}d_2, \tag{19}$$

and

$$\kappa = bC_{111} - 3aC_{112} + \frac{3a^2}{4}(C_{1122} + C_{1123}) - 3abC_{1112} + \frac{b^2}{2}C_{1111}, \tag{20}$$

$$\lambda = c_{111} + (bC_{1111} - aC_{1112}), \quad \mu = \frac{1}{2}C_{1111}.$$

Equation (17) can be reduced to a quadrature that has the analytic solution

$$G^{\pm} = 4\tilde{\kappa}(e^{\pm\sqrt{\tilde{\kappa}}(z\mp z_0)} + \Delta e^{\mp\sqrt{\tilde{\kappa}}(z\mp z_0)} + \Delta_1)^{-1}, \tag{21}$$

where $-\Delta \equiv 4\tilde{\kappa}\tilde{\mu} - \tilde{\lambda}^2$, $\Delta_1 = -2\tilde{\lambda}$, and z_0 is a constant of integration. Integration of $G^{\pm}$ gives

$$f^{\pm} = \mp\frac{2}{\sqrt{\tilde{\mu}}}\tanh^{-1}\left(\frac{e^{\pm\sqrt{\tilde{\kappa}}(z\mp z_0)} - \tilde{\lambda}}{2\sqrt{\tilde{\kappa}\tilde{\mu}}}\right) + C^{\pm}, \tag{22}$$

where $C^{\pm}$ are constants of integration.

The displacements and the strains in each material of the bilayer can be written in terms of $f^{\pm}$ and $G^{\pm}$ from Eqs. (12) and (14), respectively. Specifically, the solutions for u_z, e_1, e_3 in the material left (right) from the interface occupying the region $z < 0$ ($z > 0$) are written as

$$u_z^{L(R)} = b^{L(R)} + f^{+(-)}, \tag{23}$$

$$e_1^{L(R)} = e_{10}^{L(R)} + G^{+(-)}, \quad e_3^{L(R)} = e_{30}^{L(R)} - \frac{1}{\sqrt{3}}G^{+(-)}, \tag{24}$$

where the superscript L (R) indicates the value of the corresponding quantity in the left (right) material. For this choice, the integration constants in Eq. (22) are $C^{\pm} = \pm\frac{2}{\sqrt{\tilde{\mu}}}\tanh^{-1}(\frac{-\tilde{\lambda}}{2\sqrt{\tilde{\kappa}\tilde{\mu}}})$, so that f and its derivatives vanish on either side of the heterostructure far from the interface, in accordance with our earlier assumptions.

To obtain solutions for u_z, e_1, e_3 that are globally valid over the whole bilayer structure, we impose the following (internal) boundary conditions at the interface

$$u_z^L(z^\star) = u_z^R(z^\star), \quad \sigma_{zz}^L(z^\star) = \sigma_{zz}^R(z^\star), \tag{25}$$

where the stress component σ_{zz} is obtained from Φ_z, Eq. (10), in the static limit, and $z^\star$ is the location of the interface that is not necessarily at zero. We thus distinguish between the positions of the actual interface, where the strains exhibit significant variation, and the interface which is the natural boundary of the two materials. The actual and the natural interfaces could be slightly displaced one another due to reconstruction of the interface, similarly to that observed in Ag(111)/Ru(0001) (Ref. 36). Equation (25) can be satisfied for appropriate values of z_0 and $z^\star$ which can be obtained numerically.

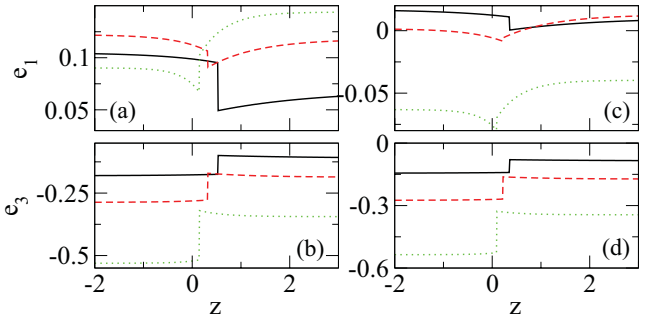

FIG. 4. (Color online) The strains e_1 and e_3 as a function of z for $c_2^L = -1$, $c_2^R = -0.76$ (black solid line), $c_2^L = -10$, $c_2^R = -7.56$ (red-dashed line); $c_2^L = -50$, $c_2^R = -37.8$ (green dotted line), and (a) , (b): $a_2^L = -31$, $a_2^R = -29.5$; (c) , (d): $a_2^L = -10$, $a_2^R = -9.5$. The other Ginzburg-Landau parameters are those for the left and the right material given in Table I.

The strains e_1 and e_3 along the z direction, that is, perpendicular to the interface, are shown in Fig. 4 for several combinations of c_2 and a_2. The strain e_1 exhibits a minimum close to the interface, indicating relative lattice compression in that region. Notably, compressionally strained layers at the $PbTiO_3/SrTiO_3$ interface, corresponding to a reduced c-axis lattice parameter of the $PbTiO_3$ film in the first few unit cells, have been experimentally observed.[35] This *interface reconstruction* is solely due to the elastic properties of the materials of the bilayer. The dependence of e_1 on z and c_2 is shown in the left panel of Fig. 5. The corresponding dependence of the well's depth, D, and the constants $z^\star$ and z_0, is shown in the right panel of Fig. 5. Thus, with decreasing c_2 (i.e., becoming more negative) D increases, while z_0, which is a measure of the well's width, decreases. Also, $z^\star$ decreases with decreasing c_2, so that the actual interface approaches the natural one at low temperatures.

The values of the Ginzburg-Landau parameters used in the calculations of the strains in Figs. 4 and 5 are given in Table I, calculated from the corresponding elastic coefficients through

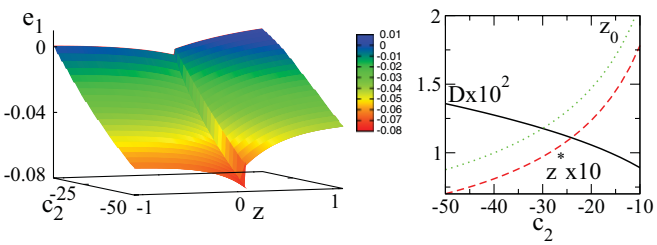

FIG. 5. (Color online) Left panel: The strain e_1 as a function of the z coordinate and the c_2 parameter. Right panel: The depth of the well D, and the numerically obtained constants z_0 and $z^\star$ as a function of c_2. The other Ginzburg-Landau parameters are those for the left and the right material given in Table I.

Eq. (4). For the left (L) material, the second- and third-order constants are those reported for $SrTiO_3$ (Refs. 32 and 32), while the second-order constants for the right (R) material are those reported recently for $LaTiO_3$ (Ref. 37). The values of the elastic coefficients, whose values are not reported in the literature due to the lack of experimental and theoretical data, are chosen to be reasonable for perovskites (Table I). However, the obtained interfacial effects persists for a wide range of values of the higher-order elastic coefficients. The strain gradient coefficients d_1 and d_2 are treated as phenomenological parameters to set the scale of the deformed region. Their values for the left and the right material are chosen to be, respectively, $d_1^L = d_2^L = 6$ and $d_1^R = d_2^R = 7$, in units of $10^{-7}N$. For this choice, significant variations in e_1 and e_3 occur within $\sim$1 nm corresponding to $\sim$2–3 TMO layers. The value of c_2 was taken to be negative for both materials, in accordance with the common practices of the Ginzburg-Landau theory of phase transitions. In Figs. 4 and 5, where c_2 and/or a_2 vary for both materials, a constant ratio between the left and the right values was assumed, calculated from their values given in Table I. The parameter a_2 is again treated phenomenologically, so that pairs of a_2^L and a_2^R with absolute values smaller that those given in Table I (but with the same ratio) have been used. These values are also consistent with the principle $e_1 \ll e_2, e_3$ for all martensitic tranformations.

It has been reported that $LaAlO_3$ and $LaTiO_3$ follow the structure of the $SrTiO_3$ substrate when the latter undergoes a CTT transition.[11,12] The correlation of these structural changes and the electromagnetic properties in these systems may be empirically seen in the observation of an enhancement in the interfacial charge carrier mobility and magnetization below T_s (Refs. 10 and 38–40). In TMO heterostructures undergoing a CTT transition, significant lattice deformation occurs at the interface region due to lattice mismatch, which results in spontaneous strains. Despite the empirical evidence for the effects of interfacial lattice deformation on the electromagnetic properties of TMO heterostructures, the relationship between the strain and the formation of a 2DEG remains largely unexplored. In a Ginzburg-Landau approach that includes charge and/or magnetic degrees of freedom, the dilatational strain e_1 couples linearly to the charge density.[41] Then the results of Fig. 4 reveal that e_1 serves as an effective potential well, which may affect the charge distribution throughout the heterostructure. In particular, the compressed interfacial region may attract and confine electron charges. The localized charges may contribute to the formation of a 2DEG, a prerequisite for interfacial metallicity in TMO heterostructures.

IV. CONCLUSION

We applied continuum elasticity to investigate theoretically the strain state of bilayer TMO heterostructures within a Ginzburg-Landau theory, and we have obtained simple approximate solutions for the fields e_1 and e_3. Interface reconstruction may lead to electronic charge redistribution in the heterostructure, and particularly to electronic charge concentration in the interface region favoring the formation of a 2DEG. The presence of a minimum in the dilatational strain field demonstrates that possibility, linking thus the elastic to the electronic properties of TMOs. Although such a reconstruction is a microscopic phenomenon involving significant changes of atomic arrangements at the interface,[21] it results in macroscopic changes of the unit cells that can be observed experimentally. Those changes can be described, at least qualitatively, by the Ginzburg-Landau theory, and their implications on the electron charge distribution of the bilayer can be inferred from basic physical laws.

ACKNOWLEDGMENTS

This work was supported by the EURYI, MEXT-CT-2006-039047, and the National Research Foundation of Singapore. We thank K. Rogdakis for useful discussions.

APPENDIX: NONLINEAR FUNCTIONS

The nonlinear functions R_i ($i = x, y, z$) are given by

$$\begin{aligned} R_x = &-a_4\left[+e_2e_3+\frac{1}{2\sqrt{3}}\left(e_2^2-e_3^2\right)\right] \\ &+\frac{b_4}{2}\left(e_2^2+e_3^2\right)\left(+e_2+\frac{1}{\sqrt{3}}e_3\right) \\ &+\frac{3a_1}{2}e_1^2+\frac{a_2}{2}\left[\left(e_2^2+e_3^2\right)+e_1\left(+e_2+\frac{1}{\sqrt{3}}e_3\right)\right] \\ &+b_1e_1^3+b_2e_1\left(e_2^2+e_3^2\right)+\frac{b_2}{2}e_1^2\left(+e_2+\frac{1}{\sqrt{3}}e_3\right) \\ &+\frac{b_7}{2}\left[e_3\left(e_3^2-3e_2^2\right)-3e_1e_2e_3+\frac{\sqrt{3}}{2}e_1\left(e_3^2-e_2^2\right)\right] \end{aligned} \tag{A1}$$

$$\begin{aligned} R_y = &-a_4\left[-e_2e_3+\frac{1}{2\sqrt{3}}\left(e_2^2-e_3^2\right)\right] \\ &+\frac{b_4}{2}\left(e_2^2+e_3^2\right)\left(-e_2+\frac{1}{\sqrt{3}}e_3\right) \\ &+\frac{3a_1}{2}e_1^2+\frac{a_2}{2}\left[\left(e_2^2+e_3^2\right)+e_1\left(-e_2+\frac{1}{\sqrt{3}}e_3\right)\right] \\ &+b_1e_1^3+b_2e_1\left(e_2^2+e_3^2\right)+\frac{b_2}{2}e_1^2\left(-e_2+\frac{1}{\sqrt{3}}e_3\right) \\ &+\frac{b_7}{2}\left[e_3\left(e_3^2-3e_2^2\right)+3e_1e_2e_3+\frac{\sqrt{3}}{2}e_1\left(e_3^2-e_2^2\right)\right] \end{aligned} \tag{A2}$$

$$\begin{aligned} R_z = &-\frac{1}{\sqrt{3}}\left[-a_4\left(e_2^2-e_3^2\right)+b_4e_3\left(e_2^2+e_3^2\right)\right] \\ &+\frac{3a_1}{2}e_1^2+\frac{a_2}{2}\left[\left(e_2^2+e_3^2\right)-\frac{2}{\sqrt{3}}e_1e_3\right] \\ &+b_1e_1^3+b_2\left[e_1\left(e_2^2+e_3^2\right)-\frac{1}{\sqrt{3}}e_1^2e_3\right] \\ &+\frac{b_7}{2}\left[e_3\left(e_3^2-3e_2^2\right)-\sqrt{3}e_1\left(e_3^2-e_2^2\right)\right]. \end{aligned} \tag{A3}$$

It can be easily checked that for $e_2 = 0$ we have $R_x = R_y$.

[1] A. Ohtomo, D. A. Muller, J. L. Grazul, and H. Y. Hwang, Nature (London) **419**, 378 (2002).
[2] A. Ohtomo and H. Y. Hwang, Nature (London) **427**, 423 (2004).
[3] K. Shibuya, T. Ohnishi, M. Kawasaki, H. Koinuma, and M. Lippmaä, Jpn. J. Appl. Phys. **43**, L1178 (2004).
[4] S. Okamoto, A. J. Millis, and N. A. Spaldin, Phys. Rev. Lett. **97**, 056802 (2006).
[5] H. Ishida and A. Liebsch, Phys. Rev. B **77**, 115350 (2008).
[6] F. J. Wong, S.-H. Baek, R. V. Chopdekar, V. V. Mehta, Ho-Won Jang, C.-B. Eom, and Y. Suzuki, Phys. Rev. B **81**, 161101(R) (2010).
[7] E. K. H. Salje, *Phase Transitions in Ferroelastic and Co-elastic Crystals* (Cambridge University Press, Cambridge, England, 1990).
[8] S. S. A. Seo, W. S. Choi, H. N. Lee, L. Yu, K. W. Kim, C. Bernhard, and T. W. Noh, Phys. Rev. Lett. **99**, 266801 (2007).
[9] J. Biscaras, N. Bergeal, A. Kushwaha, T. Wolf, A. Rastogi, R. C. Budhani, and J. Lesueur, Nat. Comms. **1**, 89 (2010).
[10] J. S. Kim, S. S. A. Seo, M. F. Chisholm, R. K. Kremer, H.-U. Habermeier, B. Keimer, and H. N. Lee, Phys. Rev. B **82**, 201407(R) (2010).
[11] K. H. Kim, D. P. Norton, J. D. Budai, M. F. Chisholm, B. C. Sales, D. K. Christen, and C. Cantoni, Phys. Status Solidi A **200**, 346 (2003).
[12] S. X. Wu, H. Y. Peng, and T. Wu, Appl. Phys. Lett. **98**, 093503 (2011).
[13] K. H. Ahn, T. Lookman, and A. R. Bishop, Nature (London) **428**, 401 (2004).
[14] A. R. Bishop, J. Phys.: Conf. Series **108**, 012027 (2008).
[15] P. Maniadis, T. Lookman, and A. R. Bishop, Phys. Rev. B **78**, 134304 (2008).
[16] C. W. Bark, D. A. Felker, Y. Wang, Y. Zhang, H. W. Jang, C. M. Folkman, J. W. Park, S. H. Baek, H. Zhou, D. D. Fong, X. Q. Pan, E. Y. Tsymbal, M. S. Rzchowski, and C. B. Eom, Proc. Natl. Acad. Sci. **108**, 4720 (2011).
[17] J. W. Seo, W. Prellier, P. Padhan, P. Boullay, J.-Y. Kim, H. Lee, C. D. Batista, I. Martin, E. E. M. Chia, T. Wu, B.-G. Cho, and C. Panagopoulos, Phys. Rev. Lett. **105**, 167206 (2010).
[18] Ho Nyung Lee, H. M. Christen, M. F. Chisholm, C. M. Rouleau, and D. H. Lowndes, Nature (London) **433**, 395 (2005).
[19] J. H. Lee, L. Fang, E. Vlahos, X. Ke, Y. W. Jung, L. Fitting-Kourkoutis, J.-W. Kim, P. J. Ryan, T. Heeg, M. Roeckerath, V. Goian, M. Bernhagen, R. Uecker, P. C. Hammel, K. M. Rabe, S. Kamba, J. Schubert, J. W. Freeland, D. A. Muller, C. J. Fennie, P. Schiffer, V. Gopalan, E. Johnston-Halperin, and D. G. Schlom, Nature (London) **466**, 954 (2010).
[20] G. C. Milward, M. J. Calderon, and P. B. Littlewood, Nature (London) **433**, 607 (2005).
[21] J. Chakhalian, J. W. Freeland, G. Cristiani, G. Khaliullin, M. van Veenendaal, and B. Keimer, Science **318**, 1114 (2007).
[22] S. Okamoto and A. J. Millis, Nature (London) **428**, 630 (2004).
[23] A. E. Jacobs, S. H. Curnoe, and R. C. Desai, Phys. Rev. B **68**, 224104 (2003).
[24] K. Ø. Rasmussen, T. Lookman, A. Saxena, A. R. Bishop, R. C. Albers, and S. R. Shenoy, Phys. Rev. Lett. **87**, 055704 (2001).
[25] A. Kosogor, V. A. L'vov, O. Söderberg, and S.-P. Hannula, Acta Mater. **59**, 3593 (2011).
[26] V. A. Chernenko and V. A. L'Vov, Philos. Mag. A **73**, 999 (1996).
[27] G. R. Barsch and J. A. Krumhansl, Phys. Rev. Lett. **53**, 1069 (1984).
[28] E. V. Gomonaj and V. A. L'Vov, Phase Transitions **47**, 9 (1994).
[29] E. V. Gomonaj and V. A. L'Vov, Phase Transitions **56**, 43 (1996).
[30] J. K. Liakos and G. A. Saunders, Philos. Mag. A **46**, 217 (1982).
[31] R. O. Bell and G. Rupprecht, Phys. Rev. **129**, 90 (1963).
[32] A. G. Beattie and G. A. Samara, J. Appl. Phys. **42**, 2376 (1971).
[33] V. A. Chernenko, M. Kohl, V. A. L'vov, V. M. Kniazkyi, M. Ohtsuka, and O. Kraft, Mater. Trans. **47**, 619 (2006).
[34] V. A. Chernenko, M. Kohl, M. Ohtsuka, T. Takagi, V. A. L'vov, and V. M. Kniazky, Mater. Sci. Eng. A **438–440**, 944 (2006).
[35] A. T. J. Helvoort, Ø. Dahl, B. G. Soleim, R. Holmestad, and T. Tybell, Appl. Phys. Lett. **86**, 092907 (2005).
[36] W. L. Ling, J. de la Figuera, N. C. Bartelt, R. Q. Hwang, A. K. Schmid, G. E. Thayer, and J. C. Hamilton, Phys. Rev. Lett. **92**, 116102 (2004).
[37] C.-M. Liu, N.-N. Ge, and G.-F. Li, Physica B **406**, 1926 (2011).
[38] M. Huijben, G. Rijnders, D. H. A. Blank, S. Bals, S. Van Aert, Jo Verbeeck, G. Van Tendeloo, A. Brinkman, and H. Hilgenkamp, Nat. Mater. **5**, 556 (2006).
[39] H. M. Christen, D. H. Kim, and C. M. Rouleau, Appl. Phys. A **93**, 807 (2008).
[40] Ariando, X. Wang, G. Baskaran, Z. Q. Liu, J. Huijben, J. B. Yi, A. Annadi, A. Roy Barman, A. Rusydi, S. Dhar, Y. P. Feng, J. Ding, H. Hilgenkamp, and T. Venkatesan, Nat. Comms. **2**, 188 (2011).
[41] A. R. Bishop, T. Lookman, A. Saxena, and S. R. Shenoy, Europhys. Lett. **63**, 289 (2003).